

## Deactivation Kinetics of Ferric Molybdate Catalysts

Y. H. MA AND S. J. KMIOTEK<sup>1</sup>

*Department of Chemical Engineering, Worcester Polytechnic Institute, Worcester, Massachusetts*

Received August 19, 1986; revised July 22, 1987

The deactivation of ferric molybdate catalysts was investigated in a differential reactor. Commercial catalysts were pretreated in air at 600 to 700°C for between 1 and 2.5 h and characterized for catalytic activity in formaldehyde synthesis and for physical and chemical properties. A kinetic model for activity decay was developed for analysis. The results indicate that on heat treatment, the active catalytic component, ferric molybdate, decomposes to an inactive phase, ferrous molybdate. © 1988 Academic Press, Inc.

### INTRODUCTION

Formaldehyde, a commodity chemical, is produced from methanol and oxygen by a process that uses an iron molybdenum oxide catalyst (1). The oxidation is highly exothermic ( $\Delta H_R = -158$  kJ/mol), and the process operates on the lean side of the explosion limit of methanol, 7 vol% in air. The catalyst is a mixture of ferric molybdate and molybdena (2). The excess molybdena is believed to assist in maintaining the molybdate structure, to add mechanical strength, and to add surface area (3). The catalyst deactivates in 6 to 12 months, largely because of sintering and molybdena volatilization at reactor hot spots.

The conversion of methanol to formaldehyde on ferric molybdate catalysts is believed to occur via a redox mechanism in what is actually an oxidative dehydrogenation. Pernicone (4) detailed the mechanism that has achieved wide acceptance. In the conversion of methanol to formaldehyde, methanol is first dissociatively chemisorbed onto the oxidized catalyst surface at Lewis acid sites. The dissociation forms a methoxy group at an anionic vacancy and a hydroxyl group. In the second step, the

catalyst is reduced with the formation of adsorbed formaldehyde and a second hydroxyl group. In the third step, the hydroxyl groups combine to form water that is desorbed. Formaldehyde then desorbs. Finally, the catalyst is reoxidized by reactant oxygen. The presence of Fe(III) is believed to increase the concentration of Lewis acid sites and increase the rates of dehydroxylation and desorption. Aside from these differences,  $\text{MoO}_3$  and  $\text{Fe}_2(\text{MoO}_4)_3$  exhibit similar kinetic behavior (5).

In a comprehensive study, Sleight and co-workers (6-10) investigated the role of many of the reaction steps. In sorption experiments, they found that methanol dissociates on the catalyst to form methoxy groups at temperatures down to room temperature. Even under these conditions, they found the hydroxyl groups to be mobile and reactive, producing water. They observed that formaldehyde and water readily desorbed. In isotope studies, they determined that extraction of hydrogen from the methoxy group was rate limiting. Furthermore, the activation energy for this step was on the order of 84.1 kJ/mol, which they found to be the activation energy for the overall reaction. Reaction rates were half order in methanol partial pressure and between zero and half order in oxygen partial pressure.

<sup>1</sup> Currently at Cabot Corporation, Billerica, MA. Work was performed at Cabot Corporation.

The only by-product observed under reaction conditions is carbon monoxide. Carbon monoxide is believed to form by continued extraction of hydrogen from the methoxy group to form CO and  $\text{H}_2\text{O}$  (11). As the extraction of hydrogen from the methoxy group is slow, CO formation is also slow, owing to the high selectivity of the catalyst. The activation energy for CO formation is reported to be 78.8 kJ/mol (11). Carbon monoxide yield is reported to increase with methanol conversion (12).

Commercial ferric molybdate catalysts deactivate in 6 to 12 months. Because the reaction is exothermic, hot spots develop. At the hot spots, molybdena volatilizes and recondenses as whiskers downstream in the reactor. There is evidence that the ferric molybdate decomposes to ferrous molybdate at the hot spots (13, 14). Aruanno (15) observed that deactivated industrial catalysts had a molybdenum-to-iron ratio of 2, whereas fresh catalysts had a ratio of 3. Pernicone (13, 14) observed that in industrial reactors, pressure drop increases, activity decreases, and formaldehyde selectivity slightly increases as deactivation progresses. At the hot spots, the catalyst sintered and surface area decreased. Molybdenum content decreased as molybdena volatilized and ferric molybdate reduced to ferrous molybdate. Electron spectroscopy for chemical analysis (ESCA) produced shoulders at 715 and 709 eV, indicating the presence of Fe(II). The Fe(III) peak occurred at 711.2 eV, the Mo(VI) peak at 232.5 eV.

Forzatti and co-workers (16, 17) proposed three kinetic models to account for deactivation. Their work was based on the deactivation of silica-supported ferric molybdate. They observed that the catalyst's activity decayed with time to a lower, non-zero value. They attributed the residual activity to residual ferric molybdate. They modeled the deactivation phenomena as the decomposition of ferric molybdate during the reaction cycle with subsequent molybdena loss. They proposed that deactivation

would not occur in the absence of reaction. The kinetic models were empirical and contained up to thirteen adjustable parameters for data fitting. The large number of adjustable parameters results in questionable statistics.

Broadly, therefore, it is the goal of this investigation to determine the nature of the deactivation process of ferric molybdate catalysts. While some work has identified physical and chemical changes in the catalyst upon deactivation, no study has determined the effect of deactivation on catalyst activity. No investigation has attempted to link physical and chemical changes in the catalyst with catalytic activity or has successfully modeled the deactivation process. Specifically, it is the objective of this investigation to quantify physical and chemical changes in the catalyst on deactivation. Furthermore, it is the objective of this investigation to relate these phenomena in a comprehensive model. To achieve these objectives, catalysts were pretreated in a microreactor in air at 600 to 700°C for between 0 and 2.5 h to simulate hot spot conditions and physical and chemical properties were determined for each sample. Differential reactor studies and a kinetic analysis were performed for each sample. A published kinetic model was used for analysis. The kinetic model was coupled with an accounting of a loss of reaction sites due to deactivation and a model for ferric molybdate decomposition.

## EXPERIMENTAL

### Apparatus

A packed bed reactor system was used for catalyst pretreatment and reaction activity studies. The flow system is shown schematically in Fig. 1. Gas flow rates were controlled with a Linde mass flow controller (FM-4450) equipped with four control modules of capacities  $0.83 \times 10^{-6}$ ,  $1.66 \times 10^{-6}$ ,  $3.32 \times 10^{-6}$ , and  $7.47 \times 10^{-6}$   $\text{m}^3/\text{s}$  air at NPT (50, 100, 200, 450 sccm). These

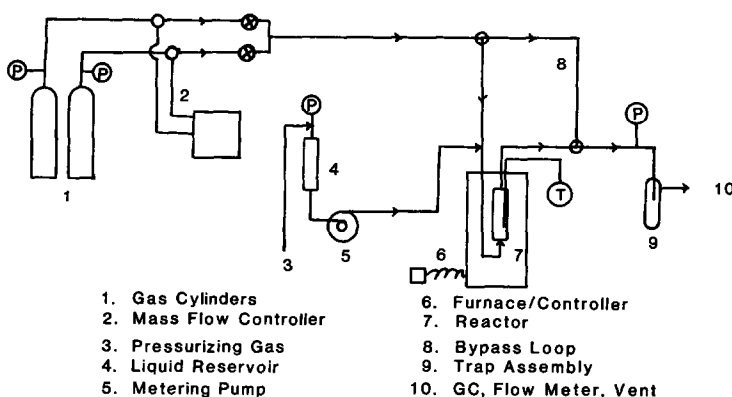


FIG. 1. Schematic diagram of reactor system.

flow rates were measured with a bubble flow meter.

Liquid flows were fed to the system by an FMI RPG6 metering pump. The pump was equipped with a 0.0032-m head with a capacity of  $6.67 \times 10^{-9} \text{ m}^3/\text{s}$  (0.125 in head, 0.4 ml/min). The stroke length of the pump was controlled with a micrometer. Liquids were fed into a cloth wick encased in a stainless steel tube. Heating tape was wrapped along the wall of the tube and a sweep gas flowed over the wick. With this technique, liquid feeds were easily and completely vaporized and transported to the reactor. The wick also damped pressure fluctuations. A  $5 \times 10^{-5} \text{ m}^3$  buret was used as a liquid reservoir, and flow rate was measured by monitoring the liquid level. The feed reservoir was pressurized with the sweep gas line to maintain a constant head.

For catalyst pretreatment studies, a 0.0127-m (0.5 in) stainless steel tube was used as a reactor (ID = 0.0094 m). The total reactor volume was  $1 \times 10^{-5} \text{ m}^3$ . The reactor was equipped with a single 0.0016-m (0.0625 in) iron-constantan (type J) thermocouple probe. This and all probes were purchased from Omega Engineering and had stainless steel sheaths. The reactor was packed with  $4.25 \times 10^{-4}$ - to  $6.00 \times 10^{-4}$ -m (30/40 mesh) catalyst particles. Reactor temperature was controlled by a Hevi-Duty split tube electric furnace with an Omega 4001 KC controller ( $100\text{--}1100^\circ\text{C} \pm 5^\circ\text{C}$ ).

For differential reactor studies, a 0.0064-m (0.25 in) OD stainless steel tube was used as a reactor (ID = 0.0038 m). The reactor was packed with  $1 \times 10^{-4}$  kg of  $4.25 \times 10^{-4}$ - to  $6.00 \times 10^{-4}$ -m (30/40 mesh) catalyst particles. The reactor was equipped with a single 0.0016-m iron-constantan thermocouple probe located at the end of the catalyst bed. Reactor temperature was controlled by a Tecam SBL-2D fluidized sand bath (fluidized with air) with a Tecam TCD4 controller ( $35\text{--}550 \pm 2^\circ\text{C}$ ). The internal dimensions of the bath were  $0.46 \times 0.23 \text{ m}$ . The reactor was placed vertically in the sand bath and reactants entered the reactor at the base of the bath. For these studies, the reactant gas was used as the sweep gas in the liquid evaporator. Pressure at the reactor outlet was measured on a USG test gauge with divisions of 13.8 kPa (2 psig).

Gas and vapor compositions were determined by an on-line HP5880A gas chromatograph. The GC was equipped with a Poropak T and a 13X molecular sieve column for  $\text{O}_2$ ,  $\text{N}_2$ ,  $\text{CO}$ ,  $\text{CO}_2$ ,  $\text{CH}_3\text{OH}$ ,  $\text{CH}_2\text{O}$ , and  $\text{H}_2\text{O}$  analysis.

## MATERIALS

### Catalysts

A commercial ferric molybdate catalyst was purchased from Harshaw Filtrol (MO-1907 T 1/8; Lot 11-Drum 19) as 0.0032-m (0.125-in.) pellets. As determined by atomic

absorption spectroscopy (AAS) (Perkin Elmer 603 AAS), the catalyst contained 9.6 wt% Fe and 57.8 wt% Mo or, expressed as oxides, 50 wt%  $\text{Fe}_2(\text{MoO}_4)_3$  and 50 wt%  $\text{MoO}_3$ . As determined by emission spectroscopy (ES) (Jarrel Ash, 3.4-m Ebert), the catalyst contained 30–300 ppm Si and 100–1000 ppm Al impurities. As determined by mercury porosimetry (Porous Materials, 15k) the pore volume was  $2.3 \text{ m}^3/\text{kg}$ , the pellet porosity was 48%, and the mean pore diameter was  $2.0 \times 10^{-7} \text{ m}$ . The solid density was  $4013 \text{ kg}/\text{m}^3$  and the apparent bulk density was  $1218 \text{ kg}/\text{m}^3$ . The BET nitrogen surface area of the catalyst was  $3860 \text{ m}^2/\text{kg}$ . The equivalent spherical diameter of the catalyst particles based on this surface area and the pellet density is  $7.8 \times 10^{-7} \text{ m}$ .

The X-ray powder diffraction (XRD) was obtained (Siemens Diffractometer with  $\text{Cu K}^\alpha$  radiation) for the catalyst. The X-ray slide was prepared by wet crushing the pellets and drying the slurry in the slide. The diffraction pattern indicated the presence of ferric molybdate and molybdenum trioxide. The  $d$ -spaces of the ferric molybdate agree well with the values reported by Fagherazzi and Pernicone (2).

The agreement between the pattern reported by these authors and the pattern

obtained in this study indicates that the as-received material was in the active catalyst form and that wet-crushing the pellets was an appropriate technique for preparing catalyst samples finer than the as-received pellets. Samples for pretreatment and differential reactor studies were prepared in this manner. Analysis of peak width data from the diffractogram indicates that the average crystallite size was  $6.0 \times 10^{-8} \text{ m}$ .

For reference, studies were also performed on reagent grade molybdena, ferric molybdate, and ferrous molybdate. All materials were purchased as powders [under  $4.4 \times 10^{-5} \text{ m}$  ( $-325$  mesh)] from Alfa. Physical data for these oxides are reported in Table I.

#### Reactants

Anhydrous, acetone-free methyl alcohol from Mallinckrodt was used as the methanol feed. The methanol contained 99.85%  $\text{CH}_3\text{OH}$  and 0.15%  $\text{H}_2\text{O}$  by weight. Reactant oxygen, sweep nitrogen, and nitrogen diluent were all UHP grade from Matheson Gas Products (99.999%).

#### Procedure

In pretreatment studies,  $1 \times 10^{-5} \text{ m}^3$  of granulated catalyst particles were loosely packed in the reactor. The reactor was

TABLE I  
Physical Data on Pure Oxides

	Oxide and lot number		
	Molybdena 110183	Ferric molybdate 111281	Ferrous molybdate 040882
Composition			
Mo (%)	68.5	50.0	45.0
Fe (%)	—	20.1	27.9
Cr (ppm)	—	1000	1000
Al (ppm)	—	500	1000
Si (ppm)	—	500	500
Ni (ppm)	—	500	500
Mn (ppm)	—	100	100
BET surface area ( $\text{m}^2/\text{kg}$ )	210	260	1200
Phase (XRD analysis)	$\text{MoO}_3 \cdot \text{H}_2\text{O}$	$\text{Fe}_2(\text{MoO}_4)_3$	$\beta\text{-FeMoO}_4$

sealed and pressure was tested. Before insertion of the reactor into the slit tube furnace, the furnace was heated to the desired temperature. With ca.  $5 \times 10^{-6}$  m<sup>3</sup>/s air at NPT flowing through it, the reactor was placed in the furnace. The reactor temperature equilibrated with the furnace temperature within 5 min. At the conclusion of the pretreatment, the reactor was removed from the furnace and allowed to cool with the air flowing through it. The reactor temperature fell to below 400°C within 5 min.

The pretreated material was removed and portions were tested for physical characteristics. There were no apparent physical differences among samples taken from different portions of the reactor. Pretreatments were performed at nominally atmospheric pressure, temperatures between 600 and 700°C, and pretreatment times of 1 to 2.5 h.

In the differential reactor studies,  $1.0 \times 10^{-4}$  kg of material was placed in the reactor. The reactor was sealed, pressure tested, and installed in the fluid sand bath. The system was heated to the desired temperature with dry feed gas flowing through it. Flow rates were chosen by the criterion proposed by Mears (18) to ensure that transport effects were negligible. Flow rates of ca.  $5 \times 10^{-6}$  m<sup>3</sup>/s were used on the basis of these criteria.

When the reactor and sand bath temperature equilibrated, the metering pump was started. Gas composition was monitored by the GC, and flow rates were monitored by the mass flow controller and the liquid level in the buret. No exotherms were observed during the course of any experiments. The steady state was achieved within 0.5 h on stream and no significant changes in product composition were observed after this time. Reactions were run under one set of conditions for a minimum of 3 h.

Differential reactor studies for the determination of formaldehyde synthesis kinetics were carried out under conditions such that the methanol conversion was under

5%. The studies were carried out between 210 and 270°C, at nominally atmospheric pressure, for residence times of ca.  $2.0 \times 10^{-2}$  s, at oxygen concentrations between 2 and 8%, at methanol concentrations between 0.5 and 5%, at water concentrations between 0 and 0.1%, and in nitrogen diluent. All concentrations are expressed in volume percentages. No conversion was observed in the absence of a catalyst.

### Reaction Kinetics

The synthesis of formaldehyde from methanol and oxygen is believed to occur via a redox mechanism (4). Jiru (21) developed a simple empirical rate expression for this mechanism. The rate expression was extended to account for water inhibition and catalyst deactivation by Forzatti and co-workers (16, 17). Unfortunately, these expressions contain several adjustable parameters.

Kmiotek (20) extended this development and gave the rate of formaldehyde production as

$$r_F = \frac{k_1 P_M^{1/2}}{1 + (k_1 P_M^{1/2} / k_2 \gamma_D P_O^{1/2}) + k_3 P_W}, \quad (1)$$

where

$$\gamma_D = \frac{(1 - \theta_D)^{1/2}}{\left(\frac{1}{1 - \theta_D}\right)^{1/2} + [1 - (1 - \theta_D)^{1/2}] \times \left[ \frac{1 + k_3 P_W}{k_1 P_M^{1/2} / k_2 P_O^{1/2}} \right]} \quad (2)$$

Here,  $r$  is reaction rate,  $P_i$  is partial pressure of  $i$ ,  $k$ 's are rate constants, and  $\theta_D$  is the fraction of sites that deactivated.

The rate repression is of the same form as the semiempirical form of Jiru (21). The half-order dependence on methanol and oxygen pressure agrees with the results of Pernicone *et al.* (22, 23) for reactant partial pressures up to 0.2 atm. Other authors, such as Sleight and co-workers (8), who used simple power law models, observed lower reaction orders for oxygen concen-

tration. As deactivation progresses, the fraction of sites deactivated increases and  $\theta_D$  decreases.

Rate constants were determined by fitting the reaction rate data for the untreated ferric molybdate catalyst to the kinetic expression by means of a least-squares analysis. For the untreated catalyst all sites were active, so the fraction of sites deactivated,  $\theta_D$ , was zero and the coefficient  $\theta_D$  had a value of unity. Values for the rate constants obtained from the analysis were

$$k_1 = 114.7 \exp(-72.8/RT) \quad \text{mol/m}^2\text{-atm}^{1/2}$$

$$k_2 = 4.350 \times 10^5 \exp(-108.8/RT) \quad \text{mol/m}^2\text{-s-atm}^{1/2}$$

$$k_3 = 7.68 \times 10^{-7} \exp(84.1/RT) \text{ atm}^{-1}$$

Activation energies are in kJ/mol.

A plot of the rate of formaldehyde synthesis as a function of oxygen and methanol partial pressures with temperature as a parameter is shown in Fig. 2. In the figure, symbols represent data points and curves represent model results. A variance analysis at the 95% confidence interval indicates that the data and the model agree to within 5%, which is within experimental error.

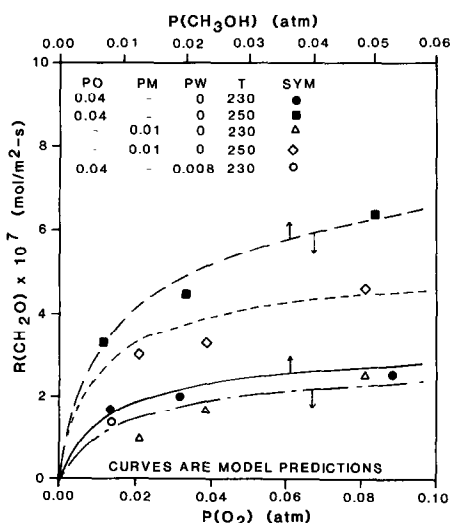


FIG. 2. Reaction rate as a function of reactant pressure; untreated catalyst.

For comparison, kinetic data were also taken on pure ferric molybdate, ferrous molybdate, and molybdena. The rate data for formaldehyde synthesis on ferric molybdate and molybdena were described well by the kinetics for formaldehyde synthesis on the Harshaw catalyst. Ferrous molybdate had no measurable activity in formaldehyde synthesis under the conditions investigated.

#### DEACTIVATION KINETICS

Both molybdena and ferric molybdate are active catalysts in formaldehyde synthesis. The fraction of sites deactivated, by definition, is

$$\theta_D = \frac{\text{sites deactivated}}{\text{original number of sites}} \quad (3)$$

Expressed in terms of the quantity of molybdena and ferric molybdate on the catalyst surface,

$$\theta_D = \frac{\alpha_D n_{\text{MoO}_3}^{\text{des}} + n_{\text{Fe}_2(\text{MoO}_4)_3}^{\text{des}}}{\alpha_D n_{\text{MoO}_3}^0 + n_{\text{Fe}_2(\text{MoO}_4)_3}^0} \quad (4)$$

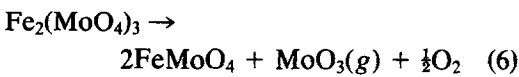
where  $n^{\text{des}}$  is the quantity (mol) of material on the surface that is destroyed,  $n^0$  is the quantity of material originally on the surface, and  $\alpha_D$  is a proportionality constant equal to the ratio of the number of sites per mole of  $\text{MoO}_3$  to the number of sites per mole of  $\text{Fe}_2(\text{MoO}_4)_3$ . Pernicone and co-workers (13) observed a direct correlation between molybdenum surface area and catalytic activity. Sleight *et al.* (24) confirmed this and concluded that every surface molybdenum atom is an active catalyst site. This implies that there are three sites per ferric molybdate molecule and one site per molybdena molecule. Thus,  $\alpha_D = 1/3$ .

The Harshaw catalyst contains, from bulk analysis, 19.9% ferric molybdate and 80.1% molybdena on a molar basis. If the surface composition is the same as the bulk composition and if the destruction of molybdena sites is very slow compared to the destruction of ferric molybdate sites,

$$\theta_D = 0.43 \frac{n_{\text{Fe}_2(\text{MoO}_4)_3}^{\text{des}}}{n_{\text{Fe}_2(\text{MoO}_4)_3}^0}, \quad (5)$$

or, when all the surface ferric molybdate is destroyed,  $\theta_D$  approaches a value of 0.43.

The nature of the deactivation is the decomposition of an active catalyst phase, ferric molybdate, to an inactive catalytic phase, ferrous molybdate. The nominal reaction describing this decomposition is



The driving force behind the transformation is the volatilization of molybdena, as dictated by the vapor pressure of molybdena. Pernicone (13) observed this transformation in deactivated catalyst pellets. Popov (25) observed this transformation even in an oxidizing atmosphere. The product of decomposition, ferrous molybdate, was reported by Trifiro and co-workers (19) and Petrini and co-workers (14) to have low activity in formaldehyde synthesis at temperatures less than 300°C. Machiels and Sleight (8) did report some activity. Kmiotek (20) observed no measurable activity at temperatures up to 270°C.

If the rate-limiting step for the decomposition reaction is the volatilization of molybdena, the rate of destruction of ferric molybdate is given by the rate of mass transfer of molybdena from the catalyst particles. The time rate of change of the ferric molybdate content in the catalyst is given by

$$\frac{dn_{\text{Fe}_2\text{Mo}_3\text{O}_{12}}}{dt} = \frac{n_{\text{Fe}_2\text{Mo}_3\text{O}_{12}}}{n_{\text{Total}}} N a_{\text{ext}} \quad (7)$$

where  $n_i$  is moles of  $i$ ,  $N$  is total molar flux,  $a_{\text{ext}}$  is external area, and  $t$  is time.

Here, the only significant flux is that of ferric molybdate. Furthermore, the flux of ferric molybdate is equal in magnitude to the flux of molybdena vapor from the surface. If the concentration of molybdena in the pellet voids is at the vapor pressure of molybdena,

$$N_{\text{MoO}_3} = k_y \left( \frac{P_{v,\text{MoO}_3} - P_{\text{MoO}_3\infty}}{P} \right) \quad (8)$$

where  $P_{v,\text{MoO}_3}$  is the vapor pressure of molybdena,  $P_{\text{MoO}_3\infty}$  is the partial pressure of molybdena in the gas phase,  $P$  is pressure, and  $k_y$  is the mass transfer coefficient. If the partial pressure of molybdena in the gas phase is negligible, combining Eqs. (7) and (8) and integrating,

$$\frac{n_{\text{Fe}_2\text{Mo}_3\text{O}_{12}}^{\text{des}}}{n_{\text{Fe}_2\text{Mo}_3\text{O}_{12}}^0} = 1 - \exp \left( \frac{-k_y a_v}{\rho_{\text{molar}}} \frac{P_{v,\text{MoO}_3}}{P} t \right) \quad (9)$$

where  $a_v$  is the volume-averaged area and  $\rho_{\text{molar}}$  is the density of the pellet.

This indicates that the quantity of ferric molybdate asymptotically approaches a value of unity. The characteristic time of the decomposition of ferric molybdate is given by the product of the vapor pressure of molybdena and the time at that condition. For small characteristic times, the quantity of ferric molybdate that decomposes is nearly linear with the characteristic time. Combining Eqs. (5) and (9) results in

$$\theta_D = 0.43 \left[ 1 - \exp \left( -k_y a_v \frac{P_{v,\text{MoO}_3}}{P} t \right) \right] \quad (10)$$

The mass transfer coefficient may be estimated from correlations in the literature or may be determined along with rate constants in the kinetic analysis.

### Results

The ferric molybdate catalyst deactivates at reactor hot spots as a result of sintering and molybdena volatilization. Because of the molybdena volatilization, ferric molybdate decomposes to ferrous molybdate. To simulate reactor hot spots, catalysts were pretreated in air at 600 to 700°C for 1 to 2.5 h. While this pretreatment cycle does not induce catalyst deactivation that would be sensitive to the reactant gas atmosphere, it permits deactivation due to surface area loss and molybdate volatilization. In this

sense, the pretreatment cycle allowed for deactivation by two mechanisms that have been proposed as the principal causes of activity loss. Ferric molybdate, ferrous molybdate, and molybdena contents in the pretreated catalyst were determined by quantitative X-ray diffraction analysis. No other phases were observed. Details of the analysis and diffraction patterns are reported in Ref. (20). A kinetic study of the formation of formaldehyde was performed on each catalyst, and the catalyst was analyzed to determine catalyst composition. In the kinetic analysis, the rate constants obtained in the analysis of rate data on the untreated catalyst were used. The only unknown in the analysis, therefore, was the fraction of sites that had deactivated,  $\theta_D$ . This parameter was obtained by fitting all the rate data for a particular catalyst to a single value of  $\theta_D$ . The kinetic testing was identical to that done on the untreated catalyst. Conditions were sufficiently mild to ensure that there was no activity loss during the kinetic testing.

It should be noted that all reaction rates were based on a unit surface area of catalyst, thereby accounting for deactivation due to surface area loss on sintering. The parameter  $\theta_D$ , therefore, represents the loss of sites due solely to the decomposition of the active phase, ferric molybdate, to the inactive phase, ferrous molybdate.

The rate of formation of formaldehyde as a function of oxygen and methanol partial

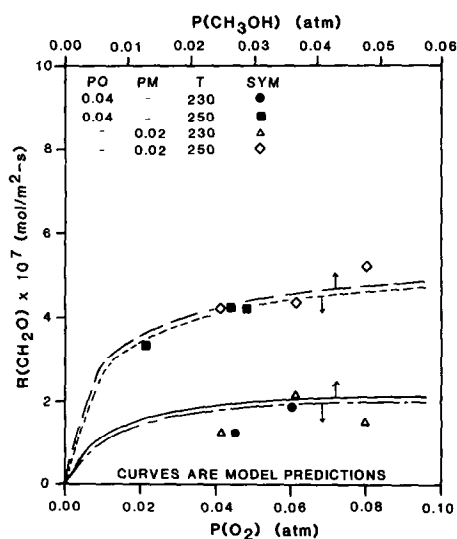


FIG. 3. Reaction rate as a function of reactant pressure; catalyst treated at 675°C for 1 h.

pressures with temperature as a parameter is shown in Fig. 3 for a catalyst that was pretreated at 675°C for 1 h. Symbols represent data points and curves represent model calculations. The value for  $\theta_D$  for this catalyst, according to a least-squares analysis, was 0.29. The excellent agreement between the data and the model indicate that the rate data can be fit to the model with rate data taken on untreated catalysts and a single value of  $\theta_D$ .

Values for  $\theta_D$  and the catalyst composition for all pretreated catalysts is given in Table 2 along with pretreatment conditions and molybdena vapor pressure under these

TABLE II  
Conditions and Results of Pretreatment Studies on Ferric Molybdate Catalysts

$T$ (°C)	$t$ (hr)	Composition (w/o)			$P_{v, \text{MoO}_3} \times 10^4$ (atm)	$\theta_D$
		$\text{Fe}_2(\text{MoO}_4)_3$	$\text{FeMoO}_4$	$\text{MoO}_3$		
600	1	51	0	49	0.11	0.11
650	1	51	0	49	0.756	0.12
650	1.5	42	6	52	0.756	0.12
650	2.5	34	10	56	0.756	0.29
675	1	34	10	56	1.88	0.29
700	1	19	21	60	4.34	0.40



conditions. Ferric molybdate, ferrous molybdate, and molybdena contents in the pretreated catalyst were determined by quantitative X-ray diffraction analysis. No other phases were observed. Details of the analysis and diffraction patterns are reported in Ref. (20). Vapor pressure data for molybdena were taken from Perry and Chilton (26). The table shows that  $\theta_D$  increased with severity of pretreatment conditions and decreased with ferric molybdate content. The value of  $\theta_D$  had values between 0 and 0.40, agreeing quite well with the predicted maximum value of 0.43.

The X-ray diffraction data indicated that untreated catalysts contained only Mo(VI) and Fe(III) in the bulk. Samples of untreated and deactivated catalysts were analyzed by ESCA to determine the chemical state of the surface molybdenum and iron. ESCA scans were performed on an untreated sample and on a catalyst treated at 675°C for 1 h. The scans indicated that the surface of the untreated catalyst contained Mo(VI) and Fe(III), whereas the surface of the pretreated catalyst contained Mo(VI), Fe(II), and lesser amounts of Fe(III).

In Figure 4,  $\theta_D$  is plotted as a function of the product of molybdena vapor pressure under the conditions of pretreatment and at the time of pretreatment. In the plot, there are two data points at  $\theta_D = 0.29$ , representing the pretreatment conditions of 650°C for

2.5 h and 675°C for 1 h. Figure 4 shows that  $\theta_D$  increases asymptotically with the product of vapor pressure and time.

According to the model, given here as Eq. (10),  $\theta_D$  is an exponential function of the vapor pressure of molybdena and time. The equation contains the constant  $k_y a_v / \rho_{\text{molar}}$ , which was obtained by least-squares fitting of the data. The value obtained for this constant was  $1.63 \text{ s}^{-1}$ .

## DISCUSSION

X-ray diffraction and ESCA data indicated the formation of ferrous molybdate on heat treatment of ferric molybdate catalyst in air. Furthermore, the catalytically inactive compound, ferrous molybdate, was the predominant iron-containing surface compound, whereas the bulk analysis indicated that most of the iron occurred as ferric molybdate. This indicates that the decomposition of ferric molybdate is a surface phenomena and that activity loss can be attributed to surface changes in the catalyst.

Catalytic activity and catalyst composition are linked through the parameter  $\theta_D$ , the fraction of sites that deactivated. The loss of active sites was proportional to the change in ferric molybdate content of the catalyst. The rate of decomposition of ferric molybdate is given by the rate of mass transfer of molybdena vapor from the catalyst and is a function only of the vapor pressure of molybdena and the time-temperature history of the catalyst.

Ideally, the mass transfer coefficient could be obtained from correlations in the literature. Catalysts were pretreated under laminar flow conditions ( $Re = 1.2$ ). Under such conditions, there is considerable scatter in mass transfer coefficient data. The literature data can be used to provide limits for the mass transfer coefficient and for comparison with observed coefficient. From mass transfer data reported by Barker (29), the mass transfer coefficient is well within the range of the predictive capa-

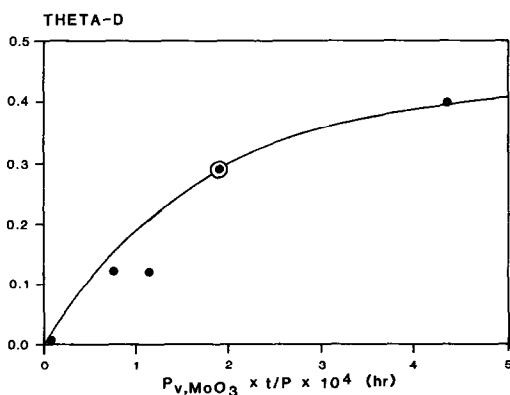


FIG. 4. Fraction of sites deactivated as a function of molybdena vapor pressure and time.

bility of the mass transfer literature. This agreement implies that the loss of reaction sites is correctly described by the rate of mass transfer of molybdena from the catalyst surface. The kinetics of this deactivation, then, can be described by physical data, vapor pressure data, and mass transfer coefficient data. No adjustable parameters are required to model the process, greatly enhancing the validity of the model.

### CONCLUSIONS

During heat treatment of ferric molybdate catalysts, ferric molybdate, an active catalytic phase in formaldehyde synthesis, decomposed to ferrous molybdate, a catalytically inactive phase. The decomposition occurred primarily on the catalyst surface and could be described by the rate of volatilization of molybdena from the surface. The loss in catalytic activity in formaldehyde synthesis could be described by the loss of ferric molybdate reaction sites on deactivation.

### ACKNOWLEDGMENT

The financial support of the Cabot Corporation is greatly appreciated.

### APPENDIX: NOMENCLATURE

$a$ :	area/volume of pellet ( $\text{m}^{-1}$ )
$a_{\text{ext}}$ :	external area ( $\text{m}^2$ )
$d_p$ :	particle diameter (m)
$\Delta H$ :	heat of reaction ( $\text{kJ/mol}$ )
$k_j$ :	rate constant for reaction $j$ ( $\text{mol/m}^2\text{-s}$ )
$n_i$ :	moles of $i$
$N$ :	molar flux ( $\text{mol/m}^2\text{-s}$ )
$P$ :	pressure (atm)
$P_i$ :	partial pressure of $i$ (atm)
$P_{v,i}$ :	vapor pressure of $i$ (atm)
$r_j$ :	reaction rate of reaction $j$ ( $\text{mol/m}^2\text{-s}$ )
$t$ :	time (s)
$T$ :	temperature ( $^{\circ}\text{C}$ )
$v$ :	velocity (m/s)
$x_i$ :	mass fraction of $i$
$y_i$ :	mole fraction of $i$

$\alpha$ :	viscosity ( $\text{kg/m-s}$ )
$\alpha_p$ :	ratio of the number of sites per mole of $\text{MoO}_3$ to the number of sites per mol $\text{Fe}_2(\text{MoO}_4)_3$
$\gamma_D$ :	deactivation coefficient defined by equation (2)
$\theta_D$ :	fraction of sites deactivated
$\rho$ :	density ( $\text{kg/m}^3$ )
$\rho_{\text{molar}}$ :	molar density of the catalyst ( $\text{mol/m}^3$ )

### Dimensionless Groups

$$\text{Re} = d_p v \rho / \mu$$

### Superscripts

o:	initial
des:	destroyed

### Subscripts

D:	deactivation
F:	formaldehyde
M:	methanol
O:	oxygen
p:	particle
W:	water
o:	initial
$\infty$ :	infinite

### REFERENCES

1. Scatterfield, C. N., "Heterogeneous Catalysis in Practice." McGraw-Hill, New York, 1980.
2. Fagherzzai, G., and Pernicone, N., *J. Catal.* **16**, 321 (1970).
3. Carbucicchio, M., and Trifiro, F., *J. Catal.* **45**, 77 (1976).
4. Pernicone, N., *J. Less-Common Met.* **36**, 289 (1974).
5. Habersberger, K., and Jiru, P., *Collect. Czech. Chem. Commun.* **37**, 535 (1972).
6. Machiels, C. J., and Sleight, A. W., *J. Catal.* **76**, 283 (1982).
7. Figueras, F., Pralus, C., Perrin, M., and Renouprez, A., *C. R. Acad. Sci. Paris* **282**, 373 (1976).
8. Machiels, C. J., Sleight, A. W., *Chem. Uses Molybdenum Proc. 4th Intl. Conf.*, p. 411 (1982).
9. Machiels, C. J., Chowdhry, V., Staley, R. H., Ohuchi, R., and Sleight, A. W., *Catal. Convers. Synth. Gas Alcohols Chem. (Proc. Symp.)*, 1983, p. 134 (1984).
10. Maciels, C. J., *ACS Symp. Ser.* **178**, 239 (1982).

11. Edwards, J., Nicolaidis, J., Cutlip, M. B., and Bennett, C. O., *J. Catal.* **50**, 24 (1977).
12. Reid, R. C., Pravsnitz, J. M., and Sherwood, T. K., "The Properties of Gases and Liquids," McGraw-Hill, New York, 1977.
13. Burriesci, N., Garbassi, F., Petrera, M., Petrini, G., and Pernicone, N., *Stud. Surf. Sci. Catal.* **6**, 115 (1980).
14. Petrini, G., Garbossi, F., Petrera, M., and Pernicone, N., *Chem. Uses Molybdenum Proc. 4th Intl. Conf.*, p. 437 (1982).
15. Aruanno, J., and Wanke, S., *Canad. J. Chem. Eng.* **55**, 93 (1977).
16. Forzatti, P., and Buzzi-Ferraris, G., *Ind. Eng. Chem. Process Des. Dev.* **21**, 67 (1982).
17. Forzatti, P., *React. Kinet. Catal. Lett.* **20**, 213 (1982).
18. Mears, D. E., *Ind. Eng. Chem. Process Des. Dev.* **10**, 541 (1971).
19. Trifiro, F., DeVecchi, V., and Pasquon, I., *J. Catal.* **15**, 8 (1969).
20. Kmiotek, S. J., Ph.D. Thesis. Worcester Polytechnic Institute, Worcester, MA, 1986.
21. Jiru, P., Wichterlova, B., and Tichy, N., *Proc. 3rd Intl. Congr. Catal., Amsterdam, 1964*, **1**, 199 (1969).
22. Pernicone, N., Lazzerin, F., Liberti, G., and Lanzavecchia, G., *J. Catal.* **14**, 293 (1969).
23. Liberti, G., Pernicone, N., and Soattini, S., *J. Catal.* **27**, 52 (1972).
24. Chang, W. H., Chowdhry, V., Ferretti, A., Firment, L. E., Groff, R. P., Machiels, C. J., McCarron, E. M., Ohuchi, F., Staley, R. H., and Sleight, A. W., *Proc. Res. Symp. Ind. Univ. Coop. Chem. Prog. Heterog. Catal.* **2**, 165 (1984).
25. Popov, B. I., Bibin, V. N., and Boreskov, G. K., *Kinet. Katal.* **17**, 371 (1976).
26. Perry, R. H., and Chilton, C. H., "Chemical Engineers' Handbook." McGraw-Hill, New York, 1973.
27. Barker, J. J., *Ind. Eng. Chem.* **57**, (1965).